Determining Chlorophyll-*a* degradation and its accuracy as a particle-tracer for bioturbation compared to luminophores

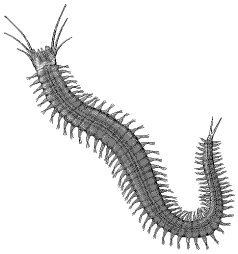

Julia van Beinum | 1998231 | MSc Research Thesis | Submitted July 2022

MSc Marine Sciences | Utrecht University | the Royal Netherlands Institute for Sea Research (NIOZ) | NIOZ Department of Estuarine & Delta Systems (EDS)

Examiners: Dr. J. Tiano and Prof. Dr. K. Soetaert

Utrecht University

NIOZ Royal Netherlands Institute for Sea Research

ABSTRACT

By mixing sediment particles, marine bioturbating animals have an essential influence on ecosystem functioning. To estimate how animals affect ecosystem functions, it is necessary to test widely used methods for accuracy and improve bioturbation quantification methods. In this study Chlorophyll-*a* (Chl-*a*) and luminophores were used as particle-tracers to quantify bioturbation rates (D_b) in muddy and sandy sediments of the Dutch Eastern Scheldt. The muddy site (Zandkreek) held 7.45 times more biomass and 3.64 times higher abundance compared to the sandy site (Dortsman). Luminophore-based bioturbation rates corresponded well with sediment oxygen consumption and the biological trait derived Bioturbation Potential index (BPc), which were all significantly higher in muddy Zandkreek. In contrast, estimated Chl-*a*-based bioturbation rates measured were not significantly different between sediment types and corresponded poorly with BPc and oxygen consumption. Also, in both sediment types Chl-*a*-based bioturbation rates were an order of magnitude higher than the luminophore-based bioturbation rates. Anaerobic Chl-*a* degradation (k_d) was 50% and 25% lower than aerobic Chl-*a* degradation in sandy and muddy sites respectfully, but the large confidence interval highlights the variability in k_d. Furthermore, k_d values in this study were an order of magnitude smaller compared to k_d values previously determined in other bioturbation studies. The variability in Chl-*a* degradation causes uncertainty in Chl-*a*-based bioturbation rates, owing to the linear scaling between the two variables in biodiffusive mixing models. Because Chl-*a* degradation varies under a range of environmental (redox) conditions, the use of Chl-*a* as a particle tracer in bioturbation quantification should, therefore, be considered with caution.

KEYWORDS

Bioturbation rates| Bioturbation potential | Chlorophyll-*a* degradation |Luminophores | Macrobenthos | Ecosystem functioning

TABLE OF CONTENTS

INTRODUCTION

Bioturbation is the reworking of particles by animals that inhabit terrestrial or marine sediment (Meysman et al., 2006). It was Charles Darwin that first described the importance of bioturbating animals, namely the bioturbating effect of worms in the soil (Darwin, 1881). Through the construction of burrows by animals and through their feeding and defecation activities (Meysman et al., 2006), bioturbation mixes sediment particles, which has a major impact on the surface of the Earth (Middelburg, 2018). The flushing of burrows with overlaying water by marine benthos increases oxygen availability and is referred to as burrow ventilation or bioirrigation (Aller, 1978; Kristensen et al., 2001).

In general, bioturbating animals are categorized as biodiffusers, gallery-diffusers, regenerators, downward conveyers or upward conveyers (François et al., 2002; Kristensen et al., 2012). Whilst biodiffusers cause random local mixing (diffusive transport) over short distances, gallery-diffusers excavate burrows causing diffusive sediment mixing near the surface and non-local mixing deeper in the sediment (François et al., 2002). Regenerators excavate burrows transferring sediment from depth to the surface causing non-local mixing. Conveyors are vertically positioned in the sediment either head-up (downward conveyers) or head-down (upward conveyers) and bring particles either down into the sediment or up towards the sediment-water interface also causing non-local mixing. In mudflat intertidal sediment often the gallery-diffuser *Hediste diversicolor* and the regenerator *Corophium volutator* are found to have a dominant influence on bioturbation (Colen, 2018).

By mixing sediment particles marine bioturbating animals act as ecosystem engineers and influence several ecosystem functions. Ecosystem engineers are animals that influence other species by modifying their mutual environment; either via their own physical structures (autogenic engineers) or by influencing the physical state of abiotic or biotic materials (allogenic engineers) (Jones et al., 1997). Bioturbating animals thus classify as both type of ecosystem engineers. Ecosystem functioning is considered the effect that species have on the transfer of energy and matter through primary and secondary production and decomposition (Boero & Bonsdorf, 2007).

Marine bioturbating macrofauna (>1mm) bring labile organic matter (OM) into the sediment, providing (microbial) fauna in the surrounding sediment with high quality OM (Middelburg, 2019). This can be considered allogenic engineering. Bioturbation also enhances bioirrigation, which leads to elevated oxygen (O_2) levels inside the sediment. Increased OM combined with increased O_2 in the sediment enhances the decomposition (degradation) of OM, which in turn results in the release of inorganic substances (remineralization) such as ammonia (Aller, 1994; Biles et al., 2002; Middelburg, 2018) which can be recycled in primary production. Benthic respiration can reflect OM degradation (Moodley & Middelburg, 1998), which is also dependent on the water temperature (Thamdrup et al., 1998). Primary producers such as phytoplankton in the water column are the base of marine foodwebs and can be dependent on the inorganic nutrients generated and released from the sediment, hence this exchange between the water column and seafloor is referred to as benthic-pelagic coupling (Griffiths et al., 2017). To summarize, bioturbation stimulates microbial activity which leads to increased inorganic nutrient release, that in turn increases primary production, thus affecting the foodweb structure of ecosystems.

Furthermore, bioturbating animals can enhance biodiversity by inducing heterogeneity. Bioturbation causes sediment properties such as permeability and stability to become heterogenous which results in a diverse topography including microclimates and niches that host a diverse animal community (Nogaro et al., 2006; Middelburg, 2019). For example, tubeworms themselves provide a habitat for sessile species which enhances biodiversity and abundance in marine benthic communities, therefore they are also referred to as foundation species (Dubois et al., 2006; Ellison, 2019). The impacts of marine bioturbating animals are not limited to ecosystem functioning, they also affect marine ecosystem services.

Whilst ecosystem functioning involves the ecological mechanisms that support ecosystems (ecosystem-centered concept), ecosystem services involve the natural processes and species that provide benefits to humankind (human-centered concept) (Brockerhoff et al., 2017). Carbon burial has the potential to remove nutrients from the water column and therefore can act as a buffer against eutrophication. When all labile organic matter inside the sediment has been processed by the animals, the remaining carbon will be buried (Middelburg, 2019). This way bioturbation aids in carbon burial and therefore provides an important ecosystem service to humankind. To be able to quantify and safeguard ecosystem functions and services that benthic macrofauna provide, as the European Union has obliged to do under the Marine Strategy Framework Directive (Directive 2008/56/EC, 17 June 2008), it is important to strive to review, improve and internationally standardize bioturbation quantification methods.

The effect of bioturbation is dependent on the size of bioturbating species, their abundance and activity. Rates of bioturbation (D_b) are usually measured by comparing the profile of a quantifiable particle-tracer to a mathematical model (Soetaert et al., 1996). However, there is no consensus regarding the methods used to quantify bioturbation rates, not regarding particle-tracers and neither regarding mathematical models (Maire et al., 2009). Natural particle tracers, such as Chlorophyll- *a* (Chl-*a*), can be used to quantify particle mixing in sediments. A pivotal issue is knowing the correct Chl-*a* degradation value (k_d) in the sediment. Chl-*a* degradation can vary, depending on the environmental conditions. For example, Chl-*a* degradation can vary with sediment grain size (Morys et al., 2016; Gogina et al., 2017) and redox conditions (Ming-Yi & Aller, 1993). Another limitation of Chl-*a* as a tracer is that sediment mixing can be biased due to selection for Chl-*a*-rich particles by benthic organisms (Mahon & Dauer, 2005). Luminophores are used as non-natural tracer particles. These are coloured sand grains that are visible under UV light and can be used as an optical tracer (Mahaut & Graf, 1987). It is unknown whether marine benthos avoid luminophore particles in the sediment whilst feeding, which could potentially cause an underestimation of bioturbation (Maire et al., 2008).

In permeable sediment oxygenated water can penetrate the sediment more easily compared to non-permeable sediments where oxygen enters the sediment through molecular diffusion driven by a concentration gradient (Ahmerkamp et al., 2017). This makes the aerobic layer in sand generally larger than in mud, which can influence oxygen consumption and thus OM and Chl-*a* degradation (Janssen & Witte, 2005; Ming-Yi & Aller, 1993). Fine-grain sediments generally receive a large quantity of OM but do not have high quality OM by definition. This is the case at 'Zandkreek', a mudflat site in the Eastern Scheldt. Sandy Eastern Scheldt site 'Dortsman' on the other hand, receives high quality OM but in lower quantities (De Borger et al., 2020).

The primary aim of this study was to compare bioturbation rates based on two different particle-tracing methods, at two contrasting sites in the Eastern Scheldt. Chl-*a* degradation was experimentally determined to be able to apply site-specific Chl-*a* k_d values to a biodiffusive mixing model. To relate bioturbation to ecosystem functioning, O_2 consumption measurements were performed and their relation to bioturbation rates was evaluated. Based on previous macrobenthic findings on the respective sites (De Borger et al., 2019) and the permeability and redox state of the sediment (Ahmerkamp et al., 2017; Ming-Yi & Aller et al., 1993), it was hypothesized to find 1) a higher benthic abundance, biomass, BPc, bioturbation rate and O2 consumption in muddy Zandkreek compared to sandy Dortsman; 2) relatively higher k_d values in aerobic and sandy conditions in contrast to anaerobic and muddy conditions; and 3) a correlation between bioturbation rates and O_2 consumption.

METHODS

Sampling

On February 18th 2022 samples were collected from two intertidal sites in the Eastern Scheldt (The Netherlands), Zandkreek (51.55354◦ N, 3.87278◦ E) and Dortsman (51.56804◦ N, 4.01425◦ E) (Fig. 1). Zandkreek is characterized by silty sediment (59 µm) and Dortsman by fine sand (140 µm) (De Borger et al., 2020). For the Chl-*a* degradation experiment six samples (⌀ 3.5 cm) of the top 2 cm of the sediment surface per site were collected, placed directly into 100 ml vials and kept on dry ice during transport to the research facility at The Royal Netherlands Institute for Sea Research, Yerseke (NIOZ-Yerseke). Three cores per site (⌀ 14.5 cm) were sampled for the determination of macrobenthic species, biomass and abundance. For the *ex-situ* bioturbation experiment involving luminophores, five sediment cores (⌀ 14.5 cm) were collected by pressing cylindrical cores into the sediment from each site. *In-situ* sediment needed to produce luminophore infused 'sediment cakes' was collected, sieved (1 mm) and dried at 60°C for 72 hours. To quantify bioturbation using Chl-*a,* an additional five sediment cores (⌀ 3.5 cm) were sampled per site.

Figure 1 | Map of the sample sites (Z) Zandkreek (51.55354◦ N, 3.87278◦ E) and (D) Dortsman (51.56804◦ N, 4.01425◦ E) in the Eastern Scheldt, the Netherlands.

Chlorophyll-*a* degradation

Twelve 100 ml vials containing 2 cm sediment (⌀ 3.5 cm) were kept for 28 days in a dark climate room at constant temperature (10°C). Six out of 12 sediment vials were sampled at Zandkreek, the other six at Dortsman. Out of the six vials per site, three vials were kept in aerobic, and three in anaerobic conditions. Vials were hand-mixed and sampled every seven days. Samples were frozen at -80°C until Chl-*a* extraction. Prior to sampling, aerobic vials were weighed to be able to replace evaporated seawater with fresh water after sampling. Anaerobic samples were handled in an anaerobic glove box.

Macrobenthos

Three sediment cores per site (⌀ 14.5 cm) were sieved (1 mm) to retain and thereafter store macrofauna in 4% buffered formalin until species identification. Animals were identified to the lowest taxonomic level possible and species abundance was recorded. Wet weights were obtained and the animals were then dried in the oven for minimal 48 hours at 65°C, after which the dry weight was measured. Biomass was oxidized at 510°C for at least three hours to obtain ash weight. Ash free dry weight (AFDW) was calculated by subtracting ash weight from dry weight.

Bioturbation

Sediment cores were transported to the research institute where they were incubated in thermostatic water tanks for 18 days with filtered (1 mm) *in-situ* seawater within temperature-controlled chambers. Seawater temperature was held constant at the average water temperature of the month (February 2022, 10°C) in which samples were retrieved. Overlying seawater was continuously aerated.

Chl-a method

To quantify bioturbation using Chl-*a*, the top 10 cm of the 10 sediment cores (⌀ 3.5 cm) collected from the field sites in February, were sliced into 0.5-cm slices (top 3 cm), 1-cm slices (3-6 cm) and 2-cm thick slices (6-10 cm). Sediment slices were frozen at -80°C for 48 hours, then freeze-dried for 72 hours and again frozen at -80°C until Chl-*a* extraction. For Chl-*a* extraction sediment samples were thawed, sieved (1 mm) and homogenized. Chl-*a* was extracted using a bullet-blender and acetone. The extracts were then placed in cuvettes for photospectometry measurements at 630, 647, 664, 665 and 750 nm.

Luminophore method

Luminophore infused sediment cakes were made by mixing luminophores with *in-situ* sediment from respective sites and seawater. The luminophore grain size does not influence sediment reworking significantly (De Backer et al., 2011), therefore, only one luminophore grain size (125 µm) was used for both sites. The luminophore-sediment mixture (1:12) was subsequently poured into a mold (⌀ 14.5 cm, 5 mm thick) and frozen at -4°C. Luminophore sediment cakes were placed on top of the 10 experimental cores at the start of the experiment. To quantify bioturbation using luminophores, 10 sediment cores (⌀ 3.5 cm) were subsampled from the 10 experimental incubation cores (⌀ 14.5 cm) after 18 days of incubation in the climate room. The top 10 cm of the sediment was sliced into 0.5-cm slices (top 3 cm), 1-cm slices (3-6 cm) and 2-cm thick slices (6-10 cm). Sediment slices were frozen at -80°C for 48 hours, then freeze-dried for 72 hours, homogenized and stored until luminophore quantification. To quantify

luminophore concentrations in the sediment, an SLR camera (Canon 1000D) with macro lens and blacklight was first used to obtain images of luminophore slices. Each slice was placed in a petri dish, lightly shaken and photographed three times to obtain a homogenized luminophore cover percentage (Appendix Fig. 1a). Luminophore pixels were then quantified in R by extracting the red band from the circle-shaped petri dish on the JPG images. As the sediment itself gives off a small amount of red-light, pixels were classified as sediment or luminophores using a red value threshold (125-250) (Wiesebron et al., 2021) (Appendix Fig. 1b). Pixels above the threshold were classified as luminophores and below the threshold as sediment. From the luminophore cover percentage the amount of luminophore pixels were calculated using the total number of pixels in the surface area of the petri dish.

Oxygen consumption

O_2 consumption measurements were performed 96 hours after sampling to allow animals to acclimatize to the climate room conditions. Each site had a control core without sediment. Before starting the measurements, the O_2 content in the overlying water was increased until near saturation (>95%) after which sediment cores were sealed by a top lid and continuously mixed by a stirrer on the inside of the top lid to homogenize the oxygen content in the seawater. The O_2 content in the water was measured every 30 seconds for a period of four hours using FireSting oxygen sensors. Oxygen saturation decrease of lower than 70% was avoided. At the end of the bioturbation experiment 18 days later O_2 consumption was measured again to check whether O_2 consumption had remained stable during the time of the experiment.

Data analyses

Statistical analyses were performed using R programming language (R version 4.1.2). Throughout the analyses a *p*-value <0.05 was considered significant. Linear regression on log-transformed Chl-*a* data was carried out per site for both aerobic and anaerobic Chl-*a* degradation. The estimates from these regressions were used as the Chl-*a* degradation k_d value in bioturbation rate calculations based on Chl-*a* and the biodiffusive mixing model of Soetaert et al. (1996) (Eq. 1). In equation 1, the Chl-*a* concentration C is defined based on a steady state diffusion equation. In fitting the Chl-*a* data, the logarithm of the concentration is plotted against the depth x. In this fit the coefficient of the slope is denoted by a. The bioturbation rate (D_b) is in $cm^{-2}\ day^{-1}$.

Equation 1 |a $$C(x) = C(0) * \exp(-\sqrt{\frac{\mathrm{k}}{\mathrm{Db}}} * x\ ).$$

Equation 1 |b $$\text{slope} = a = -\sqrt{\frac{k}{Db}}$$

Equation 1 |c $$\mathrm{Db} = -\frac{k}{a\hat{}2}$$

D_b values based on luminophore particle-tracers were obtained by fitting a biodiffusive mixing model for luminophores from the R turbo package developed by K. Soetaert and Provoost (2017). Bioturbation rates were compared between methods (Chl-*a* and luminophores) and between sites (Zandkreek and Dortsman) using a Kruskal Wallis test. O_2 consumption was calculated in $mmol\ m^{-2}\ day^{-1}$ and fitted to a linear model. Kendall's tau correlation test was used to examine the correlation between O_2 consumption and

bioturbation rates. Correlations between all variables and the grouping of species were assessed in a Principal Component Analysis (PCA), performed with centering, ln(x + 1) transformation to account for outliers, and default settings.

Bioturbation community potential (BPc), species abundance and AFDW were calculated per m^{-2} for each site. BPc was calculated as described in Solan et al. (2004) (Eq. 2). B_i is the biomass of the animal in blotted wet weight g^{-1} m^{-2}, A_i the abundance (ind. m^{-2}) and M_i and R_i the mobility and reworking score from Queirós et al. (2013) and Wrede et al. (2018). Differences in BPc, species abundance, biomass and species richness per site were examined using a Kruskal Wallis test.

Equation 2 |

$$\mathrm{BPc} = \sum_{i=1}^{n} \left(\frac{B_i}{A_i}\right)^{0.5} * A_i * M_i * R_i$$

RESULTS

Chlorophyll-*a* degradation

Chl-*a* data was log-transformed and fitted to a linear model. The slope of the regression represents the Chl-*a* degradation value k_d (day^{-1}) ± SD that is used in bioturbation rate calculations based on Chl-*a*. In anaerobic conditions in Dortsman Chl-*a* degradation was 0.004 ± 0.035 day^{-1} (F= 16.85, df= 1, *p*= 0.001) and in Zandkreek 0.003 ± 0.054 day^{-1} (n.s.) (Fig. 2a, Table 2). In Dortsman in aerobic conditions k_d was 0.008 ± 0.058 day^{-1} (F= 29.09 df= 1, *p*= 0.0001) and in Zandkreek 0.004 ± 0.096 day^{-1} (n.s.) (Fig. 2b, Table 2). Whilst in Dortsman Chl-*a* degradation was significantly faster in aerobic conditions and slower in anaerobic conditions (Chi squared= 15.23, df= 1, p< 0.001), in Zandkreek the difference between aerobic and anaerobic Chl-*a* degradation was not significant.

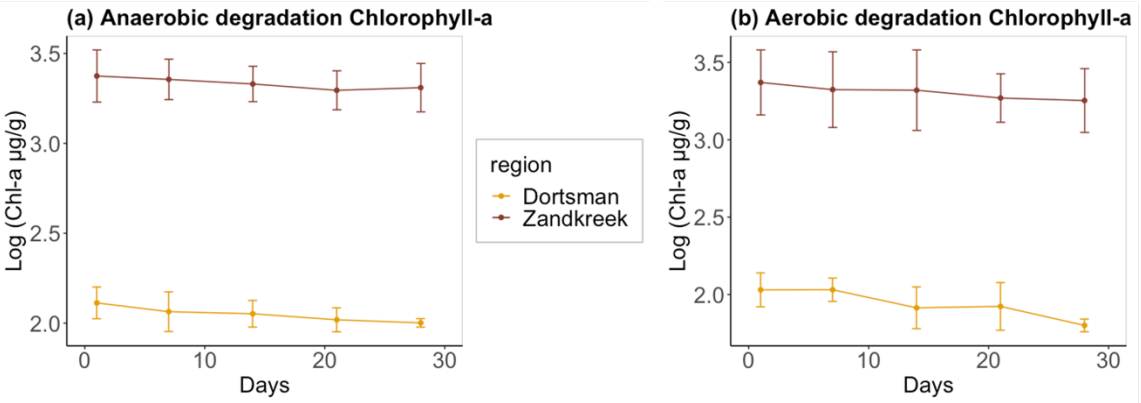

Figure 2 | Degradation of Chl-*a* in the incubated top 2 cm surface sediment for Eastern Scheldt sites Dortsman (sandy) and Zandkreek (muddy) in aerobic (n=3) and anaerobic (n=3) conditions. Error bars display a 95% confidence interval. The slope (k_d ± SD) of the linear model is for (**a**) anaerobic conditions in Dortsman 0.004 ± 0.035 day^{-1} (F= 16.85, df= 1, *p*= 0.001) and in Zandkreek 0.003 ± 0.054 day^{-1} (n.s.) (**b**) in aerobic conditions in Dortsman 0.008 ± 0.058 day^{-1} (F=29.09 df= 1, *p*= 0.0001) and in Zandkreek 0.004 ± 0.096 day^{-1} (n.s.).

Macrobenthos

In total, 13 species were found in Dortsman and 15 species in Zandkreek, of which seven species were found in both sites (Table 1). The PCA plot (Appendix Fig. 2a, b) based on

abundance displays the grouping of species per site. In Zankreek *Hediste diversicolor* explained most of the variance in the abundance data, whilst in Dortsman *Corophium sp.* did (Appendix Fig. 2a, b). The mean BPc, abundance and the biomass were higher in Zandkreek compared to Dortsman (Kruskal-Wallis H = 3.86, df= 1, p = 0.049) (Fig. 3a, b, c; Table 2). The mean (±SD) macrobenthos species richness was not significantly different between Zandkreek (7.33 ± 2.52) and Dortsman (6 ± 1) (Fig. 3d).

Table 1 | Mean (±SD) macrobenthos abundance (individuals m^{-2}) in February 2022 at Eastern Scheldt sites Dortsman and Zandkreek, excluding species that were encountered once and had insufficient AFDW weight.

Species	Zandkreek	Dortsman
Abra tenuis	65± 31	325 ± 153
Arenicola marina	-	65 ± 31
Bathyporeia	-	130 ± 61
Capitella sp.	65 ± 31	163 ± 138
Cirratulidae	98 ± 46	-
Cirratura carinata	260 ± 123	-
Corophium sp.	-	433 ± 263
Eteone sp.	65 ± 31	130 ± 61
Hediste diversicolor	2787 ± 182	65± 31
Hetromastus filiformis	65 ± 31	-
Limecola balthica	-	195 ± 92
Nematoda	65 ± 31	65 ± 31
Notomastus latericeus	195 ± 92	-
Oligochaeta	1918 ± 2620	553 ± 138
Polychaeta	-	65 ± 31
Pygospio elegans	-	130 ± 61
Ruditapes philippinarum	130 ± 61	-
Scrobicularia plana	228 ± 46	-
Spio sp.	65 ± 31	-
Spionidae	65 ± 31	65 ± 31
Streblospio sp.	130 ± 61	-

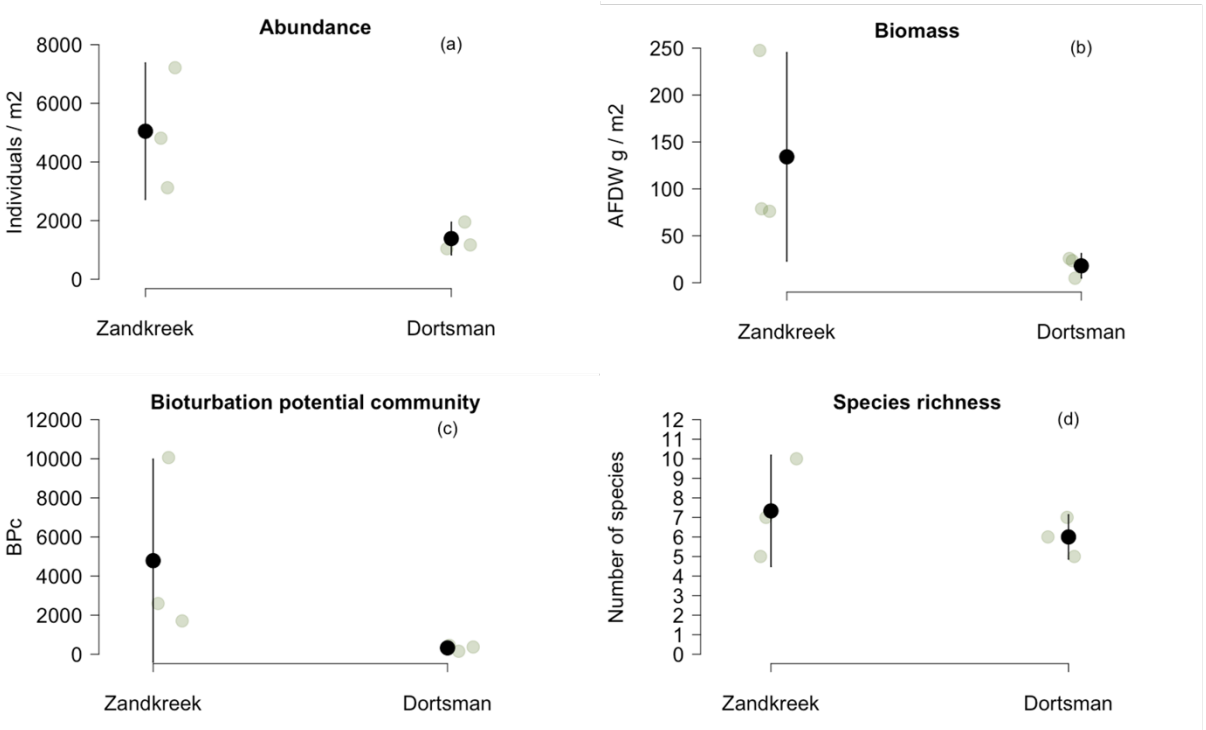

Figure 3 | **(a)** Abundance (ind. m^{-2}), **(b)** Biomass (gAFWD m^{-2}), **(c)** BPc and **(d)** Species richness for Eastern Scheldt sites Dortsman and Zandkreek in February 2022. The black dot represents the mean, the grey dots the data (n=3) and the whiskers the 95% confidence interval. Abundance, biomass and BPc were significantly higher in Zandkreek compared to Dortsman (Kruskal-Wallis H = 3.86, df= 1, p = 0.049).

Table 2 | Mean site characteristics in February 2022, displayed with the standard deviation (±SD).

Characteristic	Zandkreek	Dortsman
Abundance (ind. m^{-2}) (n=3)	5048 ± 2058	1387 ± 492
Biomass (gAFDW m^{-2}) (n=3)	134.13 ± 98.19	17.96 ± 11.50
Species richness macrobenthos (n=3)	7.33 ± 2.52	6 ± 1
BPc (n=3)	4785.68 ± 4589.21	323.03 ± 154.45
Anaerobic k_d (day^{-1}) (n=3)	0.003 ± 0.054	0.004 ± 0.035
Aerobic k_d (n=3)	0.004 ± 0.096	0.008 ± 0.058
D_b (Chl-*a*) (n=5)	0.024, ± 0.004	0.048 ± 0.027
D_b (luminophores) (n=5)	0.008 ± 0.0008	0.001 ± 0.0006
O_2 consumption (mmol m^{-2} day^{-1}) (n=5)	59.91 ± 7.69	33.97 ± 3.51

Bioturbation

The quantity of luminophores and Chl-*a* decreased with increasing depth in the sediment (Fig. 4a, b). In Dortsman, more luminophore pixels were visible in the top 3 cm (Fig. 4a) in comparison to Zandkreek. In Zandkreek, a higher quantity of Chl-*a* was present at any given depth in the entire 10 cm of sediment compared to Dortsman (Fig. 4b). Biodiffusive mixing models were fitted to the luminophore- (Fig. 5) and Chl-*a*-profile data from which the D_b values were estimated for (Fig. 6a, 6b, Table 2).

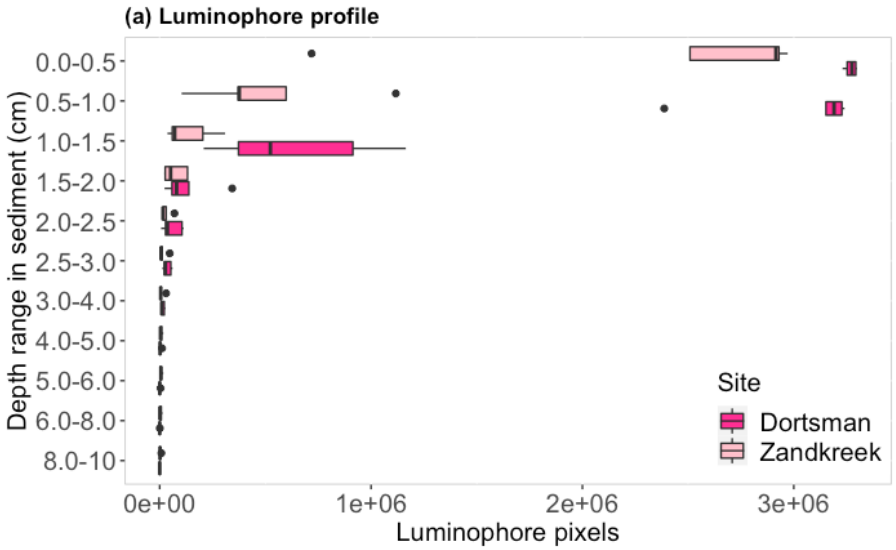

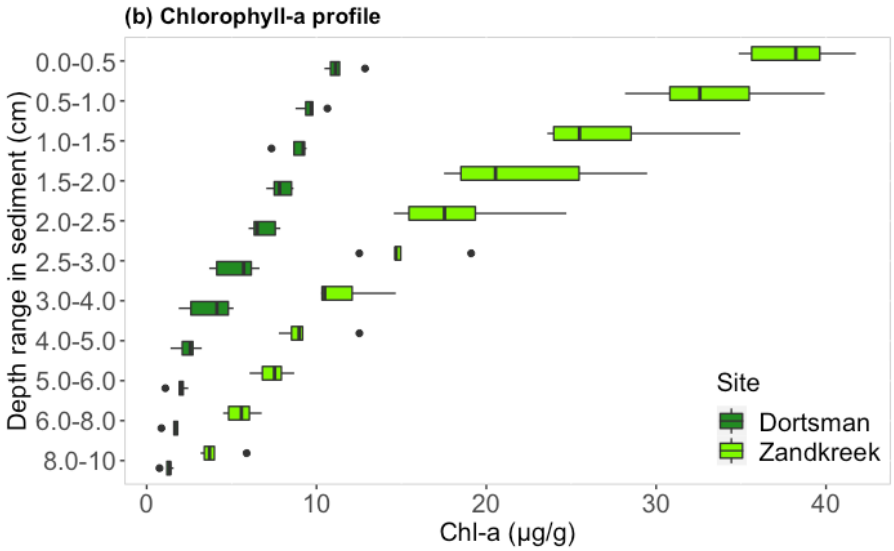

Figure 4 | Boxplots of the dispersal of **(a)** luminophore pixels per sediment slice (n=10) and **(b)** Chl-*a* (μg^{-1} g^{-1}) per sediment slice (n=10) for Eastern Scheldt sites Zandkreek and Dortsman in February 2022. The black line in the box represents the median, the box contains 25-75 % of the data, the whiskers the lowest and highest 25% of the data. Outliers are depicted as black circles.

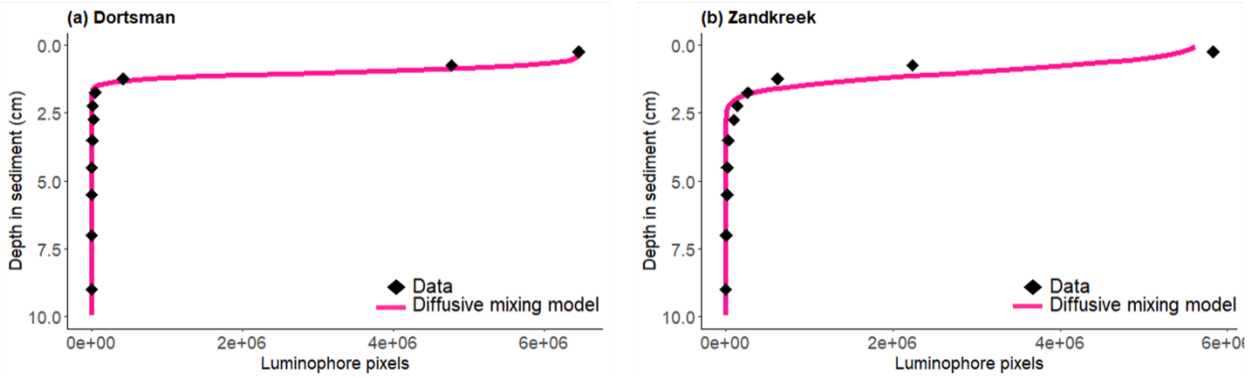

Figure 5 | Model fitting example of luminophore pixel profiles for Eastern Scheldt sites **(a)** Dortsman and **(b)** Zandkreek.

Kruskal-Wallis tests were performed to examine the differences between Chl-*a*-based D_b values and luminophore-based D_b values, and to examine differences in D_b between sites. The biodiffusive mixing model based on luminophores resulted in significantly higher D_b values in Zandkreek compared to Dortsman (Chi squared= 6.82, df= 1 p= 0.009) (Fig. 6b), whilst the biodiffusive mixing model based on Chl-*a* was not significant between sites (Fig. 6a). The mean Chl-*a*-based D_b value (±SD) was (not significantly) higher in Dortsman (0.048 ± 0.027) than Zandkreek (0.024, ± 0.004) (Table 2), but the large 95% confidence interval indicates a high uncertainty in these values. Using luminophores as a particle-tracer, the mean D_b value was higher in Zandreek (0.008 ± 0.0008) than in Dortsman (0.001 ± 0.0006) (Table 2). The D_b values based on Chl-*a* were one order of magnitude larger than the D_b values based on luminophores *a* (Chi square= 6.82, df= 1, p= 0.009) (Fig. 6a, b).

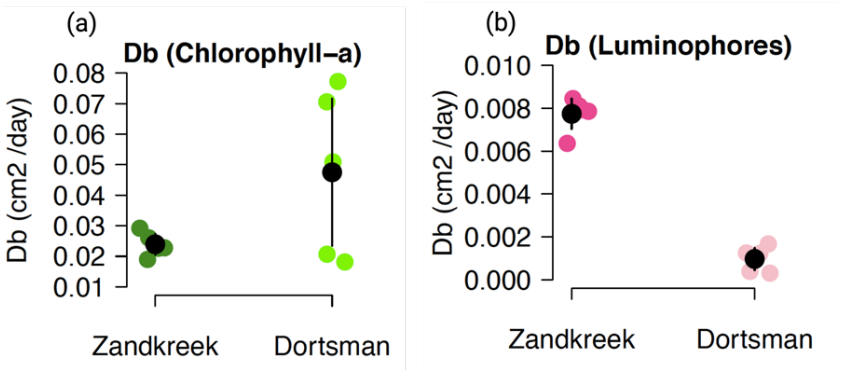

Figure 6 | Bioturbation rates by particle-tracer method for **(a)** Chl-*a* and **(b)** luminophores, from Eastern Scheldt sites Zandkreek and Dortsman in February 2022. Significantly higher D_b values in Zandkreek based on luminophores as a tracer (Chi square= 6.82, df = 1, *p*= 0.009). The black dot represents the mean, the colored dots the data (n=5) and the whiskers the 95% confidence interval.

Oxygen consumption

Kendall's tau correlation test was conducted to examine the relation between O_2 consumption and bioturbation rates (D_b). D_b correlated well with O_2 consumption for the luminophore method (tau= 0.56, p= 0.029) (Fig. 7b), but not for the Chl-*a* method (Fig. 7a). The mean (±SD) O_2 consumption (mmol m^{-2} day^{-1}) was significantly lower in Dortsman (mean= 33.97 ± 3.51) compared to Zandkreek (mean= 59.91 ± 7.69) (Table 2).

O_2 consumption correlated positively with abundance, biomass, BPc and species richness and luminophore-based D_b values (Fig. 8). Chl-*a*-based bioturbation rates negatively correlated with all variables in the dataset (Fig. 8), owing to the relatively higher Chl-*a*-based D_b values in Dortsman compared to Zandkreek (Fig. 6a, Appendix Fig. 2). O_2 consumption, species abundance and luminophore-based D_b values were well represented by the plot, whilst species richness, BPc and biomass were less represented variables (Fig. 8).

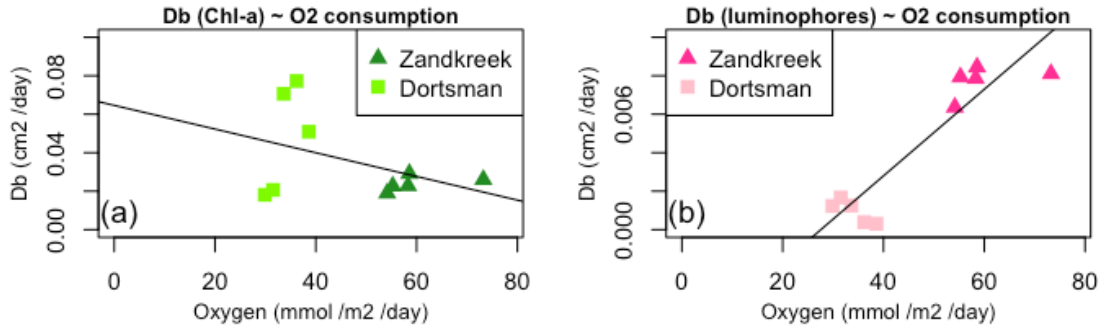

Figure 7 | Correlations between O_2 consumption (mmol m^{-2} day^{-1}) and bioturbation rates (cm^{-2} day^{-1}) (n=10). (**a**) No significant correlation between O_2 consumption and D_b based on Chl-*a* (tau= 0.56, *p*= 0.027, n=5) and (**b**) a significant correlation between O_2 consumption and D_b values based on luminophores (tau= 0.56, *p*= 0.027, n=5).

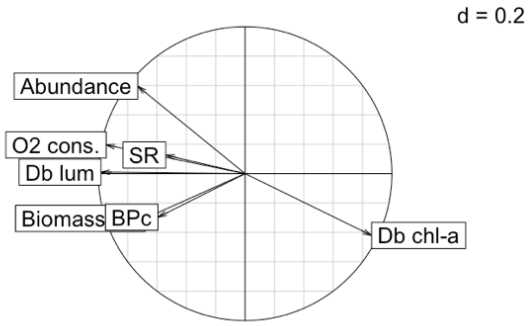

Figure 8 | Correlation circle of the PCA on bioturbation data. The smaller the angle between variables the stronger the correlation. Opposing arrows (close to 180 degrees) indicate variables are negatively correlated. An angle of 90 degrees means variables are not correlated. The length of the arrow indicates how well the plot represents the variable. PC1 and PC2 account for 63.87 % of the variance in the dataset, respectively 39.25 and 24.62 %. The 'd' states the dimension of the grid.

DISCUSSION

The results of this study show that bioturbation rates are context- and tracer-dependent, highlighting the importance of selecting a particle-tracer and comparing bioturbation rates between methods with caution. Teal et al. (2008) reports that the tracer used has a greater influence on D_b than, for example, season and water depth, leading to discrepancies in D_b values between methods. The macrobenthic selection for sediment particles with a Chl-*a*-rich coating could explain the order of magnitude difference in D_b values between methods in this study (Fig. 6) (Maire et al., 2006). Compared to Chl-*a*-poor sediment particles, macrobenthos select for Chl-*a*-rich particles 10 to 100 times more often, which increases the sediment reworking and thus D_b also by a factor 10 to 100 (Smith et al., 1993). For example, *Abra tenuis*, a bivalve species found in Dortsman, can distinguish food-poor and food-rich particles from one another which might cause an overestimation of Chl-*a*-based bioturbation rates (Hughes, 1975). Moreover, Mahon & Dauer (2005) reports Polychaetes, such as *Streblospio sp*, which were present in both Zandkreek and Dortsman, are capable of selecting specific organic compounds.

Another explanation for Chl-*a*-based D_b values being an order of magnitude higher than the luminophore-based D_b values in this study can possibly be found in the spatial variability and reactivity of Chl-*a*. This variability can be overlooked when Chl-*a* degradation, the k_d value, is assumed by the researcher and not experimentally determined. Chl-*a* degrades exponentially with time and is considered to have a relatively short half-life of 14 to 55 days, depending on the environmental conditions in the sediment (Ingalls et al., 2000). Because of this relatively fast degradation, Chl-*a* is expected to be found only at the surface of the sediment if no animals are present. Chl-*a* found below the sediment surface is a sign of bioturbation (Maire et al., 2008). However, environmental conditions e.g. sedimentation rate, turbidity, water mixing, grazing, solar radiation, water depth, temperature, chemical (redox) conditions and the abundance of microfauna all affect Chl-*a* content and degradation in the sediment (Ming-Yi & Aller et al., 1993; Szymczak-Żyła et al., 2011). For estimation of Chl-*a*-based

bioturbation rates it is, therefore, important to experimentally determine a site- or region-specific k_d value.

In this study k_d was higher in sandy Dortsman than in muddy Zandkreek, which was expected as Chl-*a* degrades faster in aerobic conditions that are more prevalent in sand than mud (Mermillod-Blondin & Rosenberg, 2006). As, hypothesized, this study found Chl-*a* degradation in anaerobic conditions to be lower than in aerobic conditions (50% and 25% lower, in sandy and muddy sites respectfully) (Fig. 2b), which agrees with the study of Szymczak-Żyła et al. (2011), that highlights anoxia results in the preservation of Chl-*a* whilst aerobic conditions stimulate the degradation of Chl-*a.* However, the 95% confidence interval displays a high uncertainty in k_d (Fig. 2), which causes uncertainty in D_b, owing to the linear scaling between the two variables (Eq. 1). Moreover, the anaerobic k_d values experimentally determined and used in this study (mud: 0.003 d^{-1}; sand: 0.004 d^{-1}) were an order of magnitude smaller than anaerobic k_d values experimentally determined by Morys et al. (2016) in the Baltic Sea (mud: 0.01 d^{-1}; sand: 0.02 d^{-1}), pointing out the variability in Chl-*a* degradation and its dependency on local environmental conditions. This variability, therefore, poses a problem in the calculation of bioturbation rates (D_b). Ingalls et al. (2000) states that Chl-*a* can have a continuum of k_d values (0.0043–0.20 d^{-1}), depending on environmental (redox) conditions, as a function of depth. Bioturbation models using Chl-*a* as a tracer may be improved by using depth dependent k_d values (potentially reflecting aerobic/anaerobic conditions) rather than a single k_d value for the entire model.

Luminophore grains have a layer of fluorescent paint and no organic coating. As is unknown whether marine benthos avoid luminophore particles whilst feeding, this could potentially underestimate D_b values based on luminophores (Maire et al., 2008), and further explain the order of magnitude difference between Chl-*a*-based and luminophore-based D_b values in this study. Another disadvantage to luminophores is that the photography involved for its quantification is time consuming. Luminophore quantification may be improved, by developing a method involving analytically quantifying luminophores through, for example, high performance liquid chromatography (HPLC). We noticed the potential of chromatography as a method for luminophore quantification during our Chl-*a* photospectometry measurements, which was also able to detect signals from luminophores in sediment slices.

Chl-*a* sediment profiles exhibited *in-situ* sediment reworking in a steady state on a seasonal timescale, whilst in this study luminophores exhibited *ex-situ* bioturbation on a shorter timescale (hours to days) (Fig. 4), which means luminophores are more suitable for short term laboratory experiments and Chl-*a* for seasonal *in-situ* experiments. Moreover, vertical Chl-*a*-profiles are in a steady state and were compared to a mathematical model with a steady state biodiffusive equation with a Chl-*a* degradation component (Eq. 1) (Soetaert et al., 1996). Modelling biodiffusive mixing with luminophore particle-tracers includes a time factor, but no degradation component. Chl-*a* and luminophores function over different time scales and operate differently, which means the selection of a particle-tracer in bioturbation quantification studies needs to be considered with caution.

From the relatively short length of the arrow in the PCA correlation plot (Fig. 8) it can be deduced that BPc was not the best represented variable to explain the bioturbation data. However, BPc did correlate well and positively with luminophore-based D_b values and O_2 consumption (Fig. 7b, Fig. 8). BPc is an indirect measure of

bioturbation which has been previously proposed to be used as a predictor for ecosystem functioning (Solan et al., 2004). BPc is based on the macrobenthic community, its biomass, abundance and traits (reworking and mobility). Although BPc does not take temporal variability, species behavior and intra- and interspecific interactions into account, it is a potential suitable measure that can be used to predict bioturbation. The BPc is also a much-needed index because bioturbation measurements based on particle-tracers are hard to come by (Teal et al., 2008; Queirós et al., 2015) whilst benthic community biological data is worldwide more readily available (Queirós et al., 2013).

BPc has been identified by some studies to correlate well with actual local and non-local bioturbation rates (Gogina et al., 2017; Morys et al., 2017), but results from other studies do not uniformly agree. Queirós et al. (2015) reports that BPc predicts bioturbation distance (random-walk model) well, but not biodiffusive transport (D_b) and bioturbation depth (*L*). Although divergent findings do not unanimously confirm the accuracy of BPc as a predictor of D_b and the datapoints in this study are few, it may be worthwhile to explore and extrapolate from the BPc and D_b values found in this study. The results from our luminophore-based bioturbation estimates suggest that D_b values may be predicted by BPc using the following model:

Equation 3 | $D_b = 7.32e\text{-}07 * BPc + 2.23e\text{-}03$

Where bioturbation (D_b) is given in $cm^{-2}d^{-1}$. We acknowledge, however, that the BPc index needs further improvements, for example in the assigning of functional groups to species, before it can be used to predict large scale bioturbation predictions (Morys et al., 2017; Queirós et al., 2013).

As hypothesized, a 3.64 times higher abundance (Fig. 3a) and 7.45 times more biomass (Fig. 3b) in Zandkreek resulted in a higher BPc (Fig 3c), luminophore-based D_b value (Fig. 6b) and O_2 consumption (Fig. 7b) in comparison to Dortsman. In Zandkreek the Chl-*a* content is almost three times as high compared to Dortsman (De Borger et al., 2020) providing macrobenthos with a high OM availability. Although the OM quality is somewhat lower in Zandkreek in comparison to Dortsman (De Borger et al., 2020) the abundant Chl-*a* in Zandkreek can enable a relatively more abundant macrobenthos community to settle (Carvalho et al., 2015). Chl-*a* depth distributions have been found to correlate well with macrofauna abundance (Morys et al., 2017). Depending on the reactivity and half-life of Chl-*a* in the sediment, Chl-*a* can reflect the bioturbation of a past period, typically between 30 and 90 days (Morys et al., 2017). Therefore, the macrobenthos identified in this study might not represent the abundance and biomass well that caused the Chl-*a* sediment reworking profile and Chl-*a*-based D_b found in this study. This could explain why the Chl-*a*-based bioturbation rate was higher in Dortsman than Zandkreek whilst the opposite was expected based on the abundance, biomass and BPc.

Furthermore, as the correlation between O_2 consumption and bioturbation rates was only significant and positive for D_b values based on luminophores (Fig. 7b), not for Chl-*a* based D_b values (Fig. 7a), this suggests the luminophore method is better suited to estimate bioturbation rates in a short-term laboratory experiment. Figure 7b displays an opposite linear trend in the data when Dortsman datapoints are considered separately, meaning there is within-site variability in the relation between O_2 consumption and D_b.

However, on a larger scale (including datapoints of both sites) there is a significant linear trend suggesting an increase in O_2 consumption can (partially) be explained by an increase in bioturbation rates (Fig. 7b). In addition to bioturbation, several other factors contribute to O_2 consumption, for example animal biomass and oxidation processes in the sediment (Glud et al., 2003).

Conclusion

The experimentally determined Chl-*a* degradation values (k_d) in this study were an order of magnitude smaller compared to k_d values previously determined in other bioturbation studies with comparable conditions (European, coastal, intertidal, marine sediment) (Bianchi & Findley, 1991; Boon & Duineveld, 1998; Ming-Yi & Aller, 1993; Morys et al., 2016). This study demonstrated that estimation of Chl-*a* degradation is context dependent because of its spatial variability and reactivity, which vary in changing environmental conditions. Because k_d scales linearly with D_b (Eq. 1), high variability in k_d causes an uncertainty in Chl-*a*-based D_b values. Therefore, if the purpose is to use Chl-*a* as a particle tracer in bioturbation quantification it is important not to assume k_d values listed in literature but to experimentally determine site- or region-specific Chl-*a* degradation rates, thus minimizing the uncertainty in Chl-*a*-based D_b values. The luminophore D_b values measured in this study corresponded much better to BPc and O_2 consumption compared to the Chl-*a*-based method, suggesting higher accuracy for luminophore-based methods when used for short-term laboratory studies. To finetune luminophore methods it is recommended to develop an analytical method for luminophore quantification. The biological data needed for BPc calculations are more readily available (Queirós et al., 2013) compared to particle-tracer-based bioturbation data (Teal et al., 2008), therefore improving the BPc index is recommend in future research. Standardizing bioturbation quantification internationally could aid in the conservation of the ecosystem functions and services that bioturbation provides.

ACKNOWLEDGEMENTS

This study was carried out at the The Royal Netherlands Institute for Sea Research (Yerseke) and counts as a partial fulfilment of a MSc Marine Sciences at Utrecht University. Gratefully acknowledged is my supervisor J. Tiano for his excellent guidance, feedback, ideas and support. I like to thank C.H. Cheng for insights on luminophore methods, G. Fivash (luminophore pixel quantification), O. Beauchard (Principal Component Analysis), D.B. Blok (species identification), M.D. Dorrestijn (feedback on mathematical aspects) and J. Brasser & Y. Maas (Chlorophyll-*a* quantification). Valuable feedback was given by K. Soetaert, P. van Breugel, A. Tramper, E. de Borger and D. Rios Yunes, for which I am thankful.

REFERENCES

Ahmerkamp, S., Winter, C., Krämer, K., Beer, D. D., Janssen, F., Friedrich, J. & Holtappels, M. (2017). Regulation of benthic oxygen fluxes in permeable sediments of the coastal ocean. *Limnology and Oceanography*, *62*(5), 1935-1954.

Aller, R. C. (1994). Bioturbation and remineralization of sedimentary organic matter: effects of redox oscillation. *Chemical Geology*, *114*(3-4), 331-345.

Bianchi, T. S., & Findlay, S. (1991). Decomposition of Hudson estuary macrophytes: photosynthetic pigment transformations and decay constants. Estuaries, 14(1), 65-73.

Biles, C. L., Paterson, D. M., Ford, R. B., Solan, M., & Raffaelli, D. G. (2002). Bioturbation, ecosystem functioning and community structure. *Hydrology and Earth System Sciences*, *6*(6), 999-1005.

Boero, F., & Bonsdorff, E. (2007). A conceptual framework for marine biodiversity and ecosystem functioning. *Marine Ecology*, *28*, 134-145.

Boon, A. R., & Duineveld, G. C. A. (1998). Chlorophyll a as a marker for bioturbation and carbon flux in southern and central North Sea sediments. *Marine Ecology Progress Series*, *162*, 33-43.

Borger, E. D., Tiano, J., Braeckman, U., Ysebaert, T., & Soetaert, K. (2020). Biological and biogeochemical methods for estimating bioirrigation: a case study in the Oosterschelde estuary. *Biogeosciences*, *17*(6), 1701-1715.

Brockerhoff, E. G., Barbaro, L., Castagneyrol, B., Forrester, D. I., Gardiner, B., González-Olabarria, J. R. & Jactel, H. (2017). Forest biodiversity, ecosystem functioning and the provision of ecosystem services. *Biodiversity and Conservation*, *26*(13), 3005-3035.

Callaway, R., Desroy, N., Dubois, S. F., Fournier, J., Frost, M., Godet, L. & Rabaut, M. (2010). Ephemeral bio-engineers or reef-building polychaetes: how stable are aggregations of the tube worm Lanice conchilega (Pallas, 1766)?. *Integrative and Comparative Biology*, *50*(2), 237-250.

Carvalho, S., Moura, A., Gaspar, M. B., Pereira, P., da Fonseca, L. C., Falcão, M. & Regala, J. (2005). Spatial and inter-annual variability of the macrobenthic communities within a coastal lagoon (Óbidos lagoon) and its relationship with environmental parameters. *Acta Oecologica*, *27*(3), 143-159.

Colen, C. V. (2018). The upper living levels: Invertebrate macrofauna. In *Mudflat Ecology* (pp. 149-168). Springer, Cham.

Cozzoli, F., Bouma, T. J., Ottolander, P., Lluch, M. S., Ysebaert, T., & Herman, P. M. (2018). The combined influence of body size and density on cohesive sediment resuspension by bioturbators. *Scientific reports*, *8*(1), 1-12.

Darwin, C. (1881) The formation of vegetable mould through the action of worms with observation on their habits. John Murray, London.

Davis, W. R. (1993). The role of bioturbation in sediment resuspension and its interaction with physical shearing. *Journal of Experimental Marine Biology and Ecology*, *171*(2), 187- 200.

De Backer, A., Van Coillie, F., Montserrat, F., Provoost, P., Van Colen, C., Vincx, M., & Degraer, S. (2011). Bioturbation effects of Corophium volutator: Importance of

density and behavioural activity. Estuarine, Coastal and Shelf Science, 91(2), 306-313.
Dubois, S., Commito, J. A., Olivier, F., & Retière, C. (2006). Effects of epibionts on Sabellaria alveolata (L.) biogenic reefs and their associated fauna in the Bay of Mont Saint- Michel. *Estuarine, Coastal and Shelf Science*, *68*(3-4), 635-646.
Ellison, A. M. (2019). Foundation species, non-trophic interactions, and the value of being common. *Iscience*, *13*, 254-268.
Directive 2008/56/EC of the European Parliament and of the Council of 17 June 2008 establishing a framework for community action in the field of marine environmental policy (Marine Strategy Framework Directive). Consulted on 28 June 2022 on https://eur-lex.europa.eu/eli/dir/2008/56/oj.
François, F., Gerino, M., Stora, G., Durbec, J. P., & Poggiale, J. C. (2002). Functional approach to sediment reworking by gallery-forming macrobenthic organisms: modeling and application with the polychaete Nereis diversicolor. *Marine Ecology Progress Series*, *229*, 127-136.
Glud, R. N., Gundersen, J. K., Røy, H., & Jørgensen, B. B. (2003). Seasonal dynamics of benthic O2 uptake in a semienclosed bay: Importance of diffusion and faunal activity. *Limnology and Oceanography*, *48*(3), 1265-1276.
Gogina, M., Morys, C., Forster, S., Gräwe, U., Friedland, R., & Zettler, M. L. (2017). Towards benthic ecosystem functioning maps: Quantifying bioturbation potential in the German part of the Baltic Sea. *Ecological indicators*, *73*, 574-588.
Griffiths, J. R., Kadin, M., Nascimento, F. J., Tamelander, T., Törnroos, A., Bonaglia, S. & Winder, M. (2017). The importance of benthic–pelagic coupling for marine ecosystem functioning in a changing world. *Global change biology*, *23*(6), 2179-2196.
Heathcote, A. J., & Downing, J. A. (2012). Impacts of eutrophication on carbon burial in freshwater lakes in an intensively agricultural landscape. Ecosystems, 15(1), 60-70.
Hughes, T. G. (1975). The sorting of food particles by Abra sp.(Bivalvia: Tellinacea). Journal of Experimental Marine Biology and Ecology, 20(2), 137-156.
Ingalls, A. E., Aller, R. C., Lee, C., & Sun, M. Y. (2000). The influence of deposit-feeding on chlorophyll-a degradation in coastal marine sediments. *Journal of marine research*, *58*(4), 631-651.
Janssen, F., Huettel, M., & Witte, U. (2005). Pore-water advection and solute fluxes in permeable marine sediments (II): Benthic respiration at three sandy sites with different permeabilities (German Bight, North Sea). *Limnology and Oceanography*, *50*(3), 779-792.
Jones, C. G., Lawton, J. H., & Shachak, M. (1997). Positive and negative effects of organisms as physical ecosystem engineers. *Ecology*, *78*(7), 1946-1957.
Kristensen, E., Penha-Lopes, G., Delefosse, M., Valdemarsen, T., Quintana, C. O., & Banta, G. T. (2012). What is bioturbation? The need for a precise definition for fauna in aquatic sciences. *Marine Ecology Progress Series*, *446*, 285-302.
Mahaut, M. L., & Graf, G. (1987). A luminophore tracer technique for bioturbation studies. *Oceanologica acta*, *10*(3), 323-328.
Mahon, H. K., & Dauer, D. M. (2005). Organic coatings and ontogenetic particle selection

in Streblospio benedicti Webster (Spionidae: Polychaeta). *Journal of experimental marine biology and ecology*, *323*(1), 84-92.

Maire, O., Duchêne, J. C., Rosenberg, R., de Mendonça Jr, J. B., & Grémare, A. (2006). Effects of food availability on sediment reworking in Abra ovata and A. nitida. *Marine Ecology Progress Series*, *319*, 135-153.

Maire, O., Lecroart, P., Meysman, F., Rosenberg, R., Duchêne, J. C., & Grémare, A. (2008). Quantification of sediment reworking rates in bioturbation research: a review. *Aquatic Biology*, *2*(3), 219-238.

Mermillod-Blondin, F., & Rosenberg, R. (2006). Ecosystem engineering: the impact of bioturbation on biogeochemical processes in marine and freshwater benthic habitats. *Aquatic sciences*, *68*(4), 434-442.

Meysman, F. J., Middelburg, J. J., & Heip, C. H. (2006). Bioturbation: a fresh look at Darwin's last idea. *Trends in Ecology & Evolution*, *21*(12), 688-695.

Middelburg, J. J. (2018). Reviews and syntheses: to the bottom of carbon processing at the seafloor. *Biogeosciences*, *15*(2), 413-427.

Middelburg, J. J. (2019). *Marine carbon biogeochemistry: A primer for earth system scientists* (p. 118). Springer Nature.

Ming-Yi, S., Lee, C., & Aller, R. C. (1993). Laboratory studies of oxic and anoxic degradation of chlorophyll-a in Long Island Sound sediments. *Geochimica et Cosmochimica Acta*, *57*(1), 147-157.

Moodley, L., Heip, C. H., & Middelburg, J. J. (1998). Benthic activity in sediments of the northwestern Adriatic Sea: sediment oxygen consumption, macro-and meiofauna dynamics. *Journal of Sea Research*, *40*(3-4), 263-280.

Morys, C., Forster, S., & Graf, G. (2016). Variability of bioturbation in various sediment types and on different spatial scales in the southwestern Baltic Sea. *Marine Ecology Progress Series*, *557*, 31-49.

Morys, C., Powilleit, M., & Forster, S. (2017). Bioturbation in relation to the depth distribution of macrozoobenthos in the southwestern Baltic Sea. *Marine Ecology Progress Series*, *579*, 19-36.

Murray, J. M., Meadows, A., & Meadows, P. S. (2002). Biogeomorphological implications of microscale interactions between sediment geotechnics and marine benthos: a review. *Geomorphology*, *47*(1), 15-30.

Nogaro, G., Mermillod-Blondin, F., François-Carcaillet, F., Gaudet, J. P., Lafont, M., & Gibert, J. (2006). Invertebrate bioturbation can reduce the clogging of sediment: an experimental study using infiltration sediment columns. *Freshwater biology*, *51*(8), 1458-1473.

Orvain, F., Le Hir, P., Sauriau, P. G., & Lefebvre, S. (2012). Modelling the effects of macrofauna on sediment transport and bed elevation: Application over a cross-shore mudflat profile and model validation. *Estuarine, Coastal and Shelf Science*, *108*, 64-75.

Queirós, A. M., Birchenough, S. N., Bremner, J., Godbold, J. A., Parker, R. E., Romero-Ramirez, A., ... & Widdicombe, S. (2013). A bioturbation classification of European marine infaunal invertebrates. Ecology and evolution, 3(11), 3958-3985.

Queirós, A. M., Stephens, N., Cook, R., Ravaglioli, C., Nunes, J., Dashfield, S., ... & Widdicombe, S. (2015). Can benthic community structure be used to predict the

process of bioturbation in real ecosystems?. *Progress in Oceanography*, *137*, 559-569.

Soetaert, K., Herman, P. M., Middelburg, J. J., Heip, C., deStigter, H. S., van Weering, T. C. & Helder, W. (1996). Modeling 210Pb-derived mixing activity in ocean margin sediments: diffusive versus nonlocal mixing. *Journal of Marine Research*, *54*(6), 1207-1227.

Soetaert, K., & Provoost, P. (2017). Turbo: functions for fitting bioturbation models to tracer data.

Solan, M., Cardinale, B. J., Downing, A. L., Engelhardt, K. A., Ruesink, J. L., & Srivastava, D. S. (2004). Extinction and ecosystem function in the marine benthos. *Science*, *306*(5699), 1177-1180.

Szymczak-Żyła, M., Kowalewska, G., & Louda, J. W. (2011). Chlorophyll-a and derivatives in recent sediments as indicators of productivity and depositional conditions. *Marine Chemistry*, *125*(1-4), 39-48.

Teal, L. R., Bulling, M. T., Parker, E. R., & Solan, M. (2008). Global patterns of bioturbation intensity and mixed depth of marine soft sediments. *Aquatic Biology*, *2*(3), 207-218.

Thamdrup, B., Hansen, J. W., & Jørgensen, B. B. (1998). Temperature dependence of aerobic respiration in a coastal sediment. *FEMS Microbiology Ecology*, *25*(2), 189-200.

Wiesebron, L. E., Steiner, N., Morys, C., Ysebaert, T., & Bouma, T. J. (2021). Sediment bulk density effects on benthic macrofauna burrowing and bioturbation behavior. *Frontiers in marine science*, *8*, 1-16.

Wrede, A., Beermann, J., Dannheim, J., Gutow, L., & Brey, T. (2018). Organism functional traitsand ecosystem supporting services–A novel approach to predict bioirrigation. *Ecological Indicators*, *91*, 737-743.

APPENDICES

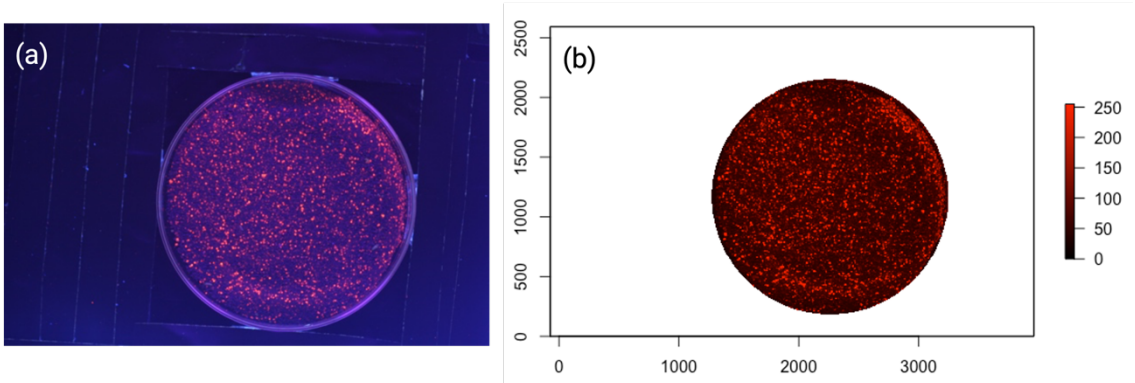

Appendix figure 1 | **(a)** JPG image taken under blacklight showing a petri dish that contains a sediment core slice with luminophores. **(b)** Pixels were classified as sediment or luminophores using a red value threshold (125 -250).

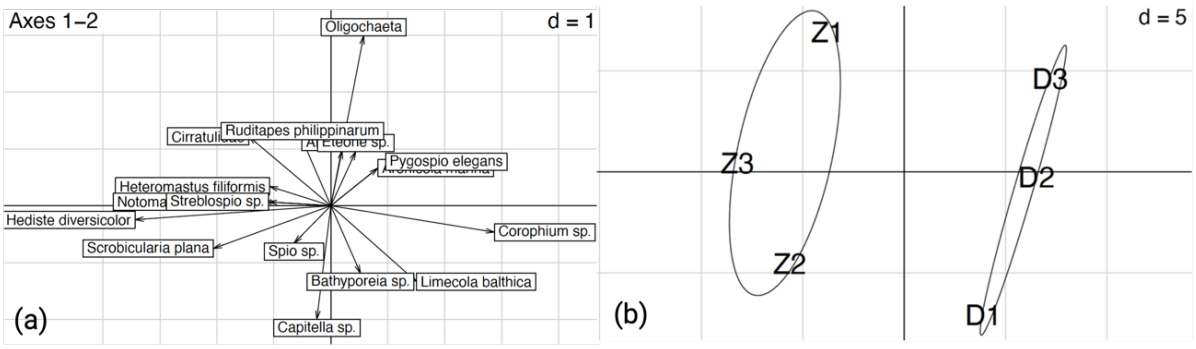

Appendix figure 2 | PCA plot on **(a)** species abundance and **(b)** the grouping op species per site. Z represents Zandkreek and D represents Dortsman, 'd' states the dimension of the grid. The length of the arrow indicates how well the species explains the variance in the abundance dataset. PC1 and PC2 account for 63.87 % of the variance in the dataset, respectively 39.25 and 24.62 %.